International Journal of Humanoid Robotics

SENSOR-BASED BIPED GAIT GENERATION SCHEME FOR HUMANOID –IMPLEMENTATION AND EVALUATION–

Kengo TODA
The Department of Integrated Information Technology,
Aoyama Gakuin University, 5-10-1 Fuchinobe, Sagaihara Kanagawa 229-8558, JAPAN
toda@it.aoyama.ac.jp

Mizuki SAGARA
Optics and Sensors Product Line, Schlumberger Company, 2-2-1 Fuchinobe, Sagamihara
Kanagawa 229-0006, JAPAN
MSagara@fuchinobe.oilfield.slb.com

Ken TOMIYAMA
The Department of Integrated Information Technology,
Aoyama Gakuin University, 5-10-1 Fuchinobe, Sagaihara Kanagawa 229-8558, JAPAN
tomiyama@it.aoyama.ac.jp

Received (Day Month Year)
Revised (Day Month Year)
Accepted (Day Month Year)

A new gait generation method, called Sensor-Based Biped Gait Generation, for humanoids is proposed here. The proposed method chooses a gait generating method from a set of prepared ones according to sensor measurements of robot's environment and to its behavior state. A gait generator that is based on the proposed method is designed and implemented onto an original humanoid to demonstrate its effectiveness.

Keywords: Biped Locomotion, Gait, ZMP, Angular Momentum

1. Introduction

The purpose of this study is to develop a biped locomotion movement generator, named the Sensor-Based Gait Generation system,[1,2] for humanoid robots that puts biped locomotion to practical use in real environment. The proposed method, in short a gait generator, enables humanoids to use various gaits according to walking surface condition. A gait generator that is based on the proposed method is designed and implemented onto an original humanoid to demonstrate effectiveness of the proposed method.

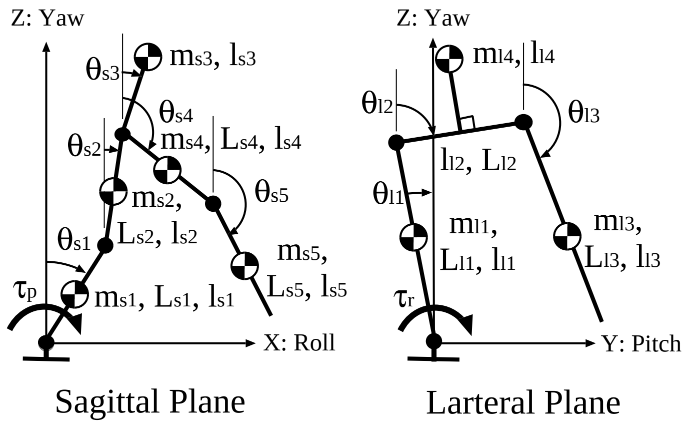

Fig. 1. Walking Model of Humanoid Robot

Human beings clearly differentiate their walking movements on the downward slope, on the slippery surface and on the flat ground. In other words, people use a gait that is appropriate to the condition of the walking surface. At present, however, humanoid robots use only a single gait with possibly adjustable parameters and therefore have clear deficiency. The proposed method imitates gait selection mechanism of human and thus eliminates this deficiency.

Many gait generation methods have been proposed already.[3,4,5,6] Each gait has good characteristics and shortcomings and therefore has advantages or disadvantages against a given walking surface condition. When humanoids adopt the proposed gait generator, robots will be able not only to walk on every road conditions but also to take advantages of good characteristics of each gait.

After explaining dynamics models of the original humanoid robot that is used in this study, the criteria for evaluation of gaits are discussed. Next, after explaining the developed and implemented system that realizes the proposed method, details of environment for experiments are described. Experimental results clearly exhibit practical advantages of the proposed method. Conclusions and items for further study are listed at the end.

2. Dynamics Models

2-D dynamics models shown in Fig. 1 are used in this study to simplify actual 3-D movement of humanoids where,

m_{si} : Mass of link i in sagittal plane (i=1∼5)
m_{lj} : Mass of link j in lateral plane (j=1∼4)
L_{si} : Length of link i in sagittal plane
L_{lj} : Length of link j in lateral plane
l_{si} : Lengh from joint to center of gravity of link i
l_{lj} : Lengh from joint to center of gravity of link j
θ_{si} : Absolute angle of link i in sagittal plane
θ_{lj} : Absolute angle of link j in lateral plane
τ_p : Ankle torque in sagittal plane
τ_r : Ankle torque in lateral plane

3. The Criteria of Evaluation

Three criteria are used to evaluate gaits and their generators. ZMP and IZMP judge degree of stability of walking,[7,8] angular momentum is adopted to check the condition (smoothness) of walk[9], and supplemented energy per step shows the energy efficiency of walk. Since ZMP, IZMP and angular momentum are used in many studies, discussions on those criteria are suppressed here and details of supplemented energy is explained below.

3.1. *Supplemented Energy*

Supplemented energy per step is the sum of consumed energy of actuators while a robot walks a step. It is obvious that smaller the supplemented energy less the lost energy. The supplemented energy is derived from the rates of changes of the positional energy and the kinetic energy. In case of a movement that has no lost energy, like a natural response of the inverted pendulum, the potential energy decreases as much as the kinetic energy increases because there is no actuation. Thus, it can be said that a movement is closer to ideal if the sum of the rate of potential energy, in short power, and the rate of kinetic energy is closer to zero.

The supplemented energy is computed with the following procedures in the sagittal plane. It is noted that, the same procedure is valid in the lateral plane with the X-axis replaced by the Y-axis and therefore the explanation of which is omitted.

- The powers by the potential energy and the kinetic energy are computed.

$$P_{ps} = \sum_{i=1}^{n} m_{si} g \dot{z}_{si} \tag{1}$$

where,

P_{ps} : Power by potential energy
g : Gravity
z_{si} : Center of gravity of link i

$$P_{ks} = \sum_{i=1}^{n} m_{si}(\ddot{x}_{si}\dot{x}_{si} + \ddot{z}_{si}\dot{z}_{si}) + I_{si}\ddot{\theta}_{si}\dot{\theta}_{si} \quad (2)$$

where,

P_{ks} : Power by kinetic energy
x_{si} : Center of gravity of link i
I_{si} : Inertia of link i

- The sum of powers is computed. Note that a positive sum implies that the total torque is applied towards the direction of walk. On the contrary, a negative sum implies that the total torque is acting on the reverse direction of walk. Here, it is assumed that the actuators of the robot have no capacity to keep energy. In either case, the total 'effort' of actuators can better be represented by the absolute value of the sum of powers and hence is used as the criterion on consumed energy here.

$$P_s = |P_{ks} + P_{ps}| \quad (3)$$

where,

P_s : Total power

- The total supplemented power per step is computed by integrating the total power over the time interval of a step.

$$E_{as} = \int_0^{T_a} P_s \, dt \quad (4)$$

where,

E_{as} : Supplemented energy in sagittal plane
T_a : Total time of a step

4. Sensor-Based Biped Gait Generation

After presenting an outline of the developed control system, elements of the developed system and each function are then described in detail.

A flowchart that shows the processing flow to and from a robot and the proposed system is given in Fig. 2. The box with dotted line represents the proposed Sensor-Based Gait Generator and consists of a gait generator and a gait library. The gait generator contains a gait selector and an interpolator. The gait library stores gait modules and a transition module. When a walk command is given to the robot, the gait selector will choose a suitable gait module according to walking surface condition and its own state that are obtained from various sensors. Next,

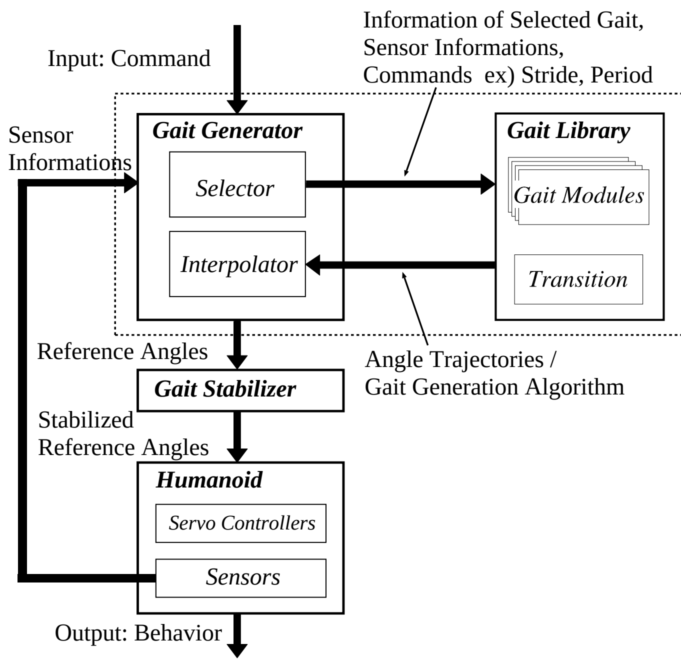

Fig. 2. Block Diagram of Control System

the interpolator generates reference angles for every joint using the selected gait module. The output of a gait generator is distributed to actuators through the compensator with possible compensations to gaits.

Elements and functions of the gait generator and the gait library are explained in detail below.

4.1. *Selector*

Selector is the central component of the proposed system and is responsible for choosing a gait from information on walk surface and on the state of the robot.

4.2. *Interpolator*

Interpolator is the gait generation engine of the system. It uses the gait module which Selector has chosen in composing angle trajectories of joints. There are two procedures to generate gaits depending on the type of walk given below.

- 1: Straight walk that can be generated in real time
- 2: Rotational and slanting gaits that can be generated in real time
- 3: Walk not suited for real time generation

In case 1, gait setting parameters, such as walk period and stride, are given to the gait module chosen by the selector and reference angles of the links are generated by the chosen gait generator. In cases 2 and 3, two angle trajectories, either pre-generate and stored or generated according to an algorithm, are compounded to form reference angles.[10]

4.3. *Gait Modules*

A gait module is a self-sustained package of a particular gait. It either contains a gait generating algorithm or a set of pre-generated gaits.

4.4. *Transition Module*

The transition module contains an algorithm for transitional movements to maintain dynamical integrity of walking when a change of gait is selected.

5. Hardware Configuration

Hardware configuration of the control system of the robot used in experiments is shown in Fig. 3.

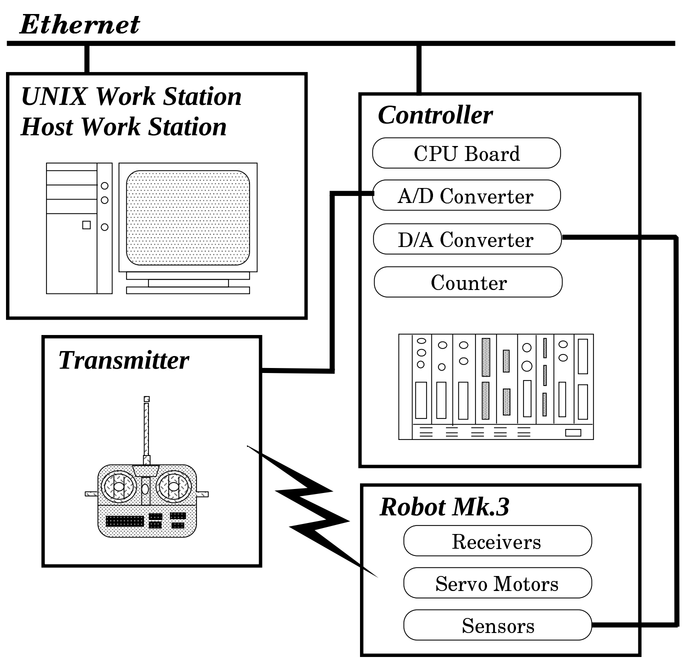

Fig. 3. Hardware Configuration for Experiments

This control system consists of a host computer, a real time controller and a biped locomotion robot Mk.3. Reference angle trajectories for links of the robot are converted into analog values with a D/A converter. The analog values are distributed wirelessly to motor modules of the robot via a transmitter and receivers. All sensor values are converted into digital value by A/D converter. The real time controller uses a commercial real time OS called VxWorks.

"The biped walking robot Mk.3 [11]" is designed by T. Furuta fro evaluation of gait generating algorithms and walk stability in 1998. Figure 4 is a view of Mk.3, Fig. 5 shows the distribution of degrees of freedom.

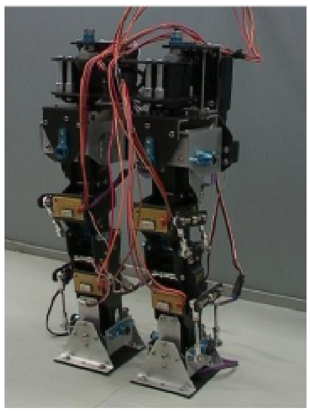

Fig. 4. Mk.3

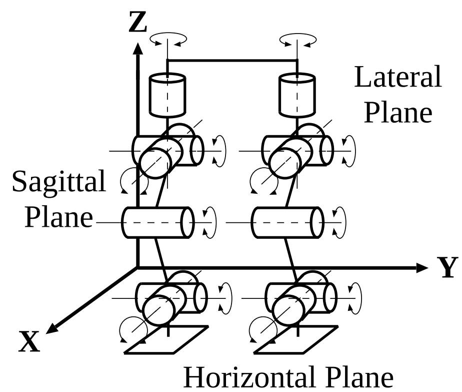

Fig. 5. DOF Distribution of Mk.3

6. Experimental System

The developed and implemented system that realizes the proposed method is explained. Especially this section concentrates on gait modules, the selector and the transition module. The interpolator is not mentioned since the structure of this part does not change with specification of experiment changes.

6.1. *Gait Modules*

Three kinds of gait modules, gait by the "Multi-linked inverted pendulum method[5]", the "multi-phase gait[6]" generating method and a gait for static walk are constructed and stored in the experimental system. Although the multi-linked inverted pendulum method has the smallest energy consumption, adjustments of body movement is difficult since there is no double-leg supporting phase. The stability of this method therefore is established only on level grounds. On the contrary, robots with the multi-phase gait generator can continue walking on rough grounds within limits since adjustments of movements during the double-leg supporting phase is possible. However, energy consumption is comparatively large. The static walk has the highest stability margin and can walk through rough grounds within a larger limit than the multi-phase gait. Since the walk cycle is long, however, the walk speed is low and energy consumption is large.

6.2. *Selector*

Selection and change of gait are performed every two steps at the start of the walk cycle. The reason for every two steps is that gait transition at every step implies that the gait selection of next step must be done while the transient effect of gait change is still prevailing and this will cause errors in selection of gaits. The selection of gait follows the flow chart shown in Fig. 6.

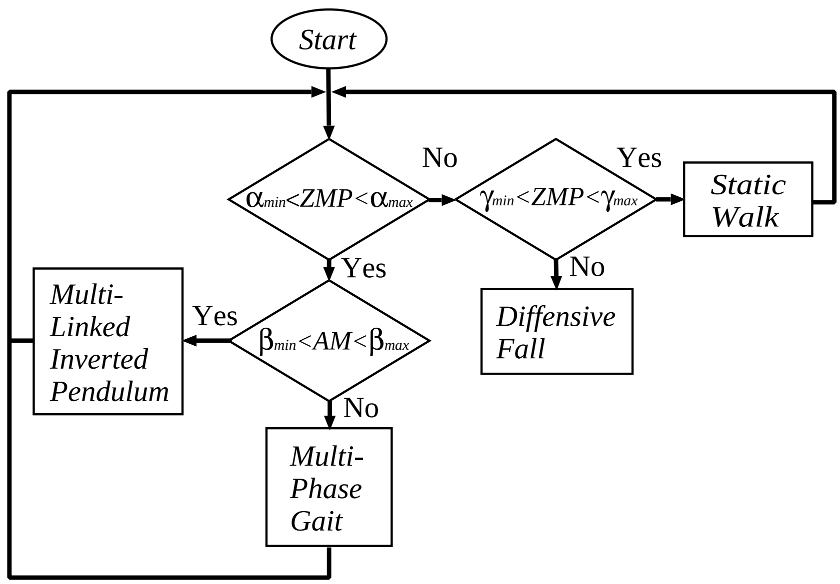

Fig. 6. Flow Chart of Gait Selection

Gyroscope sensors on each leg link and universal six-axis force sensors installed between sole and foot are used. Measurement of angular momentum (AM) is from gyroscope sensors and measurement of ZMP is from universal force sensors. Measured values are used for judgment at gait selection brunch points.

At the gait selection, the system first obtains a measured ZMP and determines walk stability margin. If the ZMP deviation is over a threshold $(\alpha_{min}, \alpha_{max})$, imminence of falling is judged first. Defensive fall is selected if the stability margin of ZMP equals zero. Otherwise, static walk is selected because it is the most stable walk. If ZMP deviation is in an intermediate band defined by the thresholds $(\alpha_{min}$ and $\alpha_{max})$, then the next gait is selected based on the angular momentum. It is noted that the angular momentum is an index that can express degree of rotational motion of a robot, just as ZMP is an index that is able to determine the condition of contact between sole and grounds. Therefore, magnitude of the forward motion of a humanoid can best be evaluated by the angular momentum. Since there is an appropriate range of the angular momentum for steady walk, the measured angular momentum is tested if it lies within a set of thresholds β_{min} and β_{max}. If that is the case, then Multi-linked inverted pendulum method is selected as the gait generator. If the angular momentum is out of the threshold, multi-phase gait that is more stable than the Multi-link inverted pendulum method is selected as the next gait by the selector. It is known that the values used in this criteria are very sensitive and are affected by even microscopic ground conditions. The sensitivity of gait selection can be reduced by elimination of high-frequency components of the sensed data. Averages of the sensor values over 0.080 second intervals preceding the gait selection is used for this purpose. A weak point of this operation is the possibility of missing a sharp maximum of ZMP and, as a result, missing the onset of instability. However, this can be overcome by adopting enough stability margin through tactically chosen thresholds α_{min} and α_{max}. The following set of threshold values is used: (5)∼(10).

$$\alpha_{min} = -6.0 \quad [mm] \tag{5}$$
$$\alpha_{max} = 10 \quad [mm] \tag{6}$$
$$\beta_{min} = -0.15 \quad [kgm^2/sec] \tag{7}$$
$$\beta_{max} = -0.030 \quad [kgm^2/sec] \tag{8}$$
$$\gamma_{min} = -40 \quad [mm] \tag{9}$$
$$\gamma_{max} = 40 \quad [mm] \tag{10}$$

Here, the threshold α is set at 16 [mm] that is 20% of 80[mm], the actual sole length in traveling direction of our original robot. In addition, thresholds α_{min} and α_{max} are shifted forward by 2[mm]. It is because the vertical projection of the center of gravity deviates 2[mm] in the forward direction with our robot. γ_{min} and γ_{max} are set at 40 [mm], sole edge positions, because they represent the limit of stability. For the case of the thresholds of angular momentum, they should be decided based on the desired values derived from the planned motion. However, we determined the thresholds based on preliminary experiments consisting of several walking tests on the level ground. The reason for this is a hardware problem. We found that backlashes at gears of the robot have adverse effects on the measured angular momentum through these experiments. It is noted that those thresholds depend only on robot hardware parameters such as the size of sole, accuracy of sensors, and other physical parameters and not on environmental conditions. Environmental conditions are taken into consideration through measurements and switching gaits.

The design approach for Selector based on both ZMP and the angular momentum discussed above is a sufficiently general and valid one. The developed Selector should be applicable to many robots and gaits. However, more conditional branchings based on not only ZMP and the angular momentum but also some combinations of them may be necessary depending on such factors as a robot hardware, types of gaits and criteria for robot motion evaluation. The fundamental reason for the lack of a general design procedure is that the selection of gait is inherently rooted in factors such as hardware specifications and characteristics of each gait.

6.3. *Transition Module*

The transition module generates motions in the double-leg supporting phase for connecting gaits before and after this phase. Trajectories of the waist joint in both sagittal and lateral planes are determined first from positions and speeds of the waist joint at the end of the prior gait and the start of the new gait. Then, this information is used to generate all other joint angle trajectories. It is noted that this transition operation is to be completed within 0.40[*sec*].

The waist joint trajectory is designed using cubic polynomials as shown in (11)∼(13). Note that those trajectories make position and speed of the waist joint at the start and the end continuous. Both the initial and final conditions of the waist joint trajectory are determined from the supporting leg, which is the hind leg for the initial condition and the fore leg for the final condition. This is because the position and the speed of the waist joint looking from the support-leg expresses the absolute speed of the robot trunk.

$$x_w(t) = \alpha_{x1} + \alpha_{x2}t + \alpha_{x3}t^2 + \alpha_{x4}t^3 \tag{11}$$

$$y_w(t) = \alpha_{y1} + \alpha_{y2}t + \alpha_{y3}t^2 + \alpha_{y4}t^3 \tag{12}$$

$$z_w(t) = \alpha_{z1} + \alpha_{z2}t + \alpha_{z3}t^2 + \alpha_{z4}t^3 \tag{13}$$

where,

t :	Time
$x_w(t)$:	Position of waist at time t
$y_w(t)$:	Position of waist at time t
$z_w(t)$:	Position of waist at time t
α_{xn} :	Coefficients of cubic polynomial (n=1∼4)
α_{yn} :	Coefficients of cubic polynomial
α_{zn} :	Coefficients of cubic polynomial

The waist joint trajectories shown in (11)∼(13) are used to compute angle trajectories of links in the sagittal plane. Here, the upper body is vertically fixed in order to prevent large movement of the center of gravity. The angle orbit of each

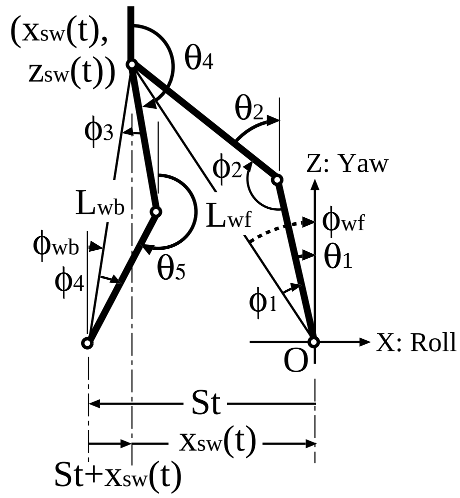

Fig. 7. Movement While Transition

link can be determined using (14)∼(18) from geometrical constraints representing kinematics configuration of the robot. The same procedure is also applicable in the lateral plane.

$$\theta_{s1}(t) = \phi_{wf}(t) + \phi_1 \tag{14}$$
$$\theta_{s2}(t) = \theta_1(t) + \phi_2 - \pi \tag{15}$$
$$\theta_{s3}(t) = 0.00 \tag{16}$$
$$\theta_{s4}(t) = \phi_{wb}(t) - \phi_3 + \pi \tag{17}$$
$$\theta_{s5}(t) = \phi_{wb}(t) + \phi_4 + \pi \tag{18}$$

where,

$\theta_{si}(t)$: Angle orbit of link i in sagittal plane
St : Stride
L_{wf} : Length parameter for computation of the fore leg
L_{wb} : Length parameter for computation of the hind leg
ϕ_{wf} : Angle parameter for computation of the fore leg
ϕ_{wb} : Angle parameter for computation of the hind leg
ϕ_k : Angle parameter for computation (k=1∼4)

$$\theta_{l1}(t) = \cos^{-1}\frac{z_w(t)}{L_{l1}} \tag{19}$$
$$\theta_{l2}(t) = \frac{\pi}{2} \tag{20}$$
$$\theta_{l3}(t) = \theta_{l1}(t) + \pi \tag{21}$$

where,

$$\theta_{lj}(t): \quad \text{Angle orbit of link } j \text{ in lateral plane}$$

7. Experiments

Two purposes of this experiment are evaluation of the developed experimental system and demonstration of effectiveness of the proposed method.

7.1. *Experimental Set-ups*

The developed system is implemented onto the control system of the biped locomotion robot Mk.3.[11] The robot is commanded to walk on a changing road surface. In the first case, the surface changes from an upward slope with angle of $5[deg]$ to an yielding surface (covered with two sheets of cardboard). In the second case, the surface changes from a flat horizontal ground to an upward slope with angle of $5[deg]$. The robot is commanded to walk at least ten steps in both cases.

During the evaluation experiments, ZMP and angular momentum are measured. At the same time, information on gait selection and overall operation are obtained. The collected data is used for verification of intended operation of the developed experimental system. Next, success rate of planned walk, amount of the supplemented energy and traversal time to complete the commanded walk are compared between the proposed method and conventional single gait generation scheme in order to evaluate effectiveness of the proposed method. Major parameter values used for gait generation are listed in Table 1.

Table 1. Parameter Settings of Each Gait

Gait	Stride $[m]$	Period $[sec]$
Static Walk	0.050	2.0
Multi-Phase Gait	0.050	0.70
Multi-Linked IP	0.050	0.80

7.2. *Result of the Verification Experiments*

Typical trajectories of gait selection, the measured angular momentum and the ZMP from one each of two cases are shown in Result I (Fig. 8) and Result II (Fig. 9). Blue lines in the top figures show the selection of gaits. Middle graph is the angular momentum. The lowermost graph is the measured ZMP. Values shown in yellow are the instantaneous measurement of sensors and the red curves are the running average over the $0.080[sec]$ time duration and are used as indices of gait selection. Green dotted lines show the maximum and minimum thresholds. Vertical dashed lines point the timing of gait selection.

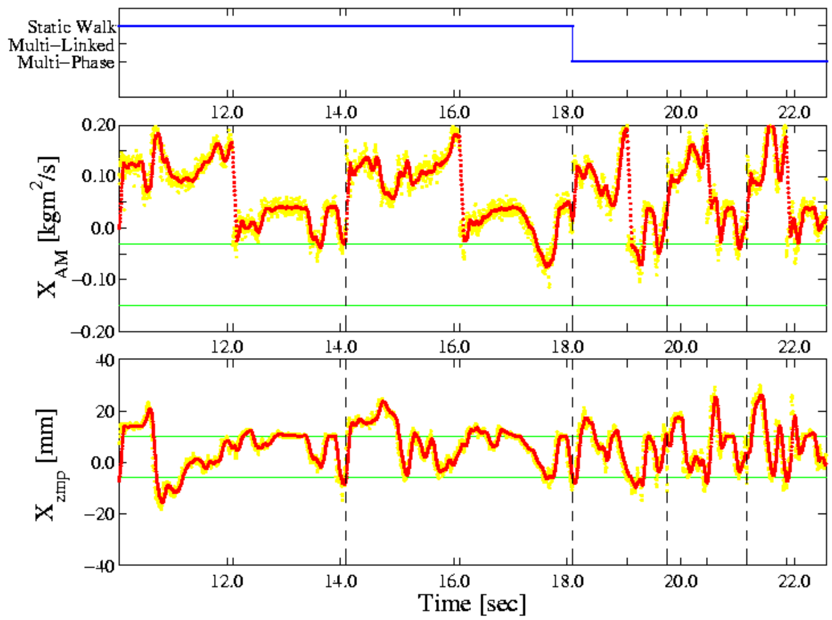

Fig. 8. Gait Selection and Sensor Values I: Walking through an upward slope with angle of 5[deg] and encountering an yielding surface at time 18.1[sec]

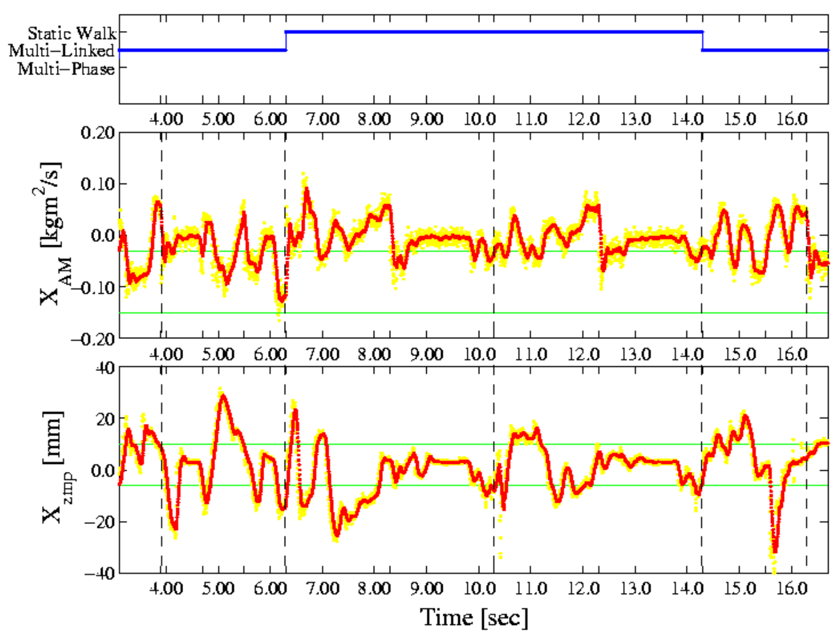

Fig. 9. Gait Selection and Sensor Values II: Walking through a flat horizontal ground and encountering an upward slope at time 6.30[sec]

In Result I, at the first and second gait selection timings (10.1[*sec*], left end of the graph and 14.1[*sec*]), static walk is chosen because the averaged ZMP deviates from the range of thresholds. The robot moves onto the yielding surface at the third timing (18.1[*sec*]) of gait selection. The ZMP comes back within the limits of the threshold at this timing but the angular momentum stays outside of the threshold. It is observed that the selected gait is changed to the multi-phase gait in response to this. In summary, the static walk with the highest stability margin is chosen on the upward slope and the multi-phase gait is chosen on the yielding surface based on a comparatively wider stability margin.

In Result II, the gait of multi-linked inverted pendulum method is chosen on the initial horizontal ground since the ZMP and the angular momentum are judged to be within the limits of the thresholds. At the second gait selection timing (6.30[*sec*]) when the robot proceeds to the upward slope, the ZMP deviated out of the threshold. Therefore, static walk with highest stability is chosen. At the fourth timing (14.3[*sec*]) of gait selection, the gait of multi-linked inverted pendulum method is chosen since the angular momentum returns within the threshold and then the commanded walk is completed. This result exhibits the gait selection corresponding to the road surface condition is realized using sensor information.

7.3. *Effectiveness of the Proposed Method*

The sensor-based gait generation and conventional single gait generation are compared. Comparisons of the success rate of walking, traversal time and supplemented energy are shown in Table 2, Table 3 and Table 4, respectively. In Table 2, the upper three success rates of static, multi-phased and multi-linked gaits are the averages of success rates on the two experimental walk surfaces mentioned above. The cases marked Sensor-Based Gait I and II in those tables correspond to two walk surface cases in the last subsection.

In Sensor-Based I (corresponding to Result I), the rate of successful completion of commanded walk is improved compared with the multi-phase gait and the gait of multi-linked inverted pendulum method only cases. Moreover, the traversal time of walk is shortened compared with the static walk. In Sensor-Based II (corresponding to Result II), the success rate of walk is also improved compared with the multi-phase gait and multi-linked inverted pendulum and the traversal time of walk is also shortened compared with the static walk. Moreover, the supplemented energy is reduced compared with those of the multi-phase gait and the static gait.

The high success rate of walk comparable to the static gait only case, however, is not obtained in neither of the experiments. The major cause of this is the instability during the transition from a gait to another. This indicates the necessity to improve the scheme used in the transition phase. By doing this, success rates equivalent to static walk can be expected in sensor-based gait I and II. It is also noted that it is impossible to decrease supplemented energy of the sensor-based gait less than that of the multi-linked inverted pendulum method. This is because the sensor-based gait uses walking stability, not the supplemented energy, as the criteria for walk selection. It is also noted that the success rate is no more than 80% even for the case of static gait in the series of experiments. The reason for this is that no balance control is implemented in the experiments in order to evaluate effects of gait change only. The experimental result also shows that the supplemented energy and the traversal time of walk are both reduced without reducing the success rate of walk. Therefore, it can be concluded that the humanoid can acquire sufficient mobility and can make full use of the advantages of each gait.

Table 2. Success Rate of Each Gait

Gait	Success Rate
Static Gait	16/20
Multi-Phase Gait	7/20
Multi-Linked IP	3/20
Sensor-Based Gait I	10/20
Sensor-Based Gait II	10/20

Table 3. Traversal Time of Each Gait

Gait	Time [*sec*]
Static Gait	20.0
Multi-Phase Gait	7.00
Multi-Linked IP	8.00
Sensor-Based Gait I	12.4
Sensor-Based Gait II	13.2

Table 4. Supplemented Energy of Each Gait

Gait	E_{as} [Nm]	E_{al} [Nm]
Static Gait	0.94	1.0
Multi-Phase Gait	1.2	0.70
Multi-Linked IP	0.49	0.42
Sensor-Based Gait I	1.0	0.90
Sensor-Based Gait II	0.68	0.85

8. Conclusion

A Sensor-Based Gait Generation method is devised and an experimental system was built. Moreover, this system is implemented onto an original humanoid robot to evaluate operations and demonstrate effectiveness of the proposed method. Experimental result exhibits successful gait selection corresponding to road surface environment from sensor information. Additionally, the supplemented energy and total time of walking are both reduced without reducing the success rate of walking.

Future studies targeting to improving the success rate include improvement of the transition scheme for changing gait generation method, developing and implementing the compensator and addition of more gait modules. There also is a room for improvements in the design procedure for the gait module selector although adding a new gait generation module is a straightforward task. For improving the transition for gait changing, a technique of making gait change more gradually and dynamically less burdening to joints would be effective.

References

Proceedings:

1. S. Yashiro et al. Real-Time Gait Generation Based on Sensor Information and Nominal Gaits (in Japanese), in *2002 JSME Conf. on Robotics and Mechatronics (ROBOMEC)* (2002), 1P1-E07 (CDROM).

Proceedings:

2. M. Sagara et al. Sensor-Based Biped Gait Generation for Humanoid (in Japanese), in *The 20th Annual Conference of the Robotics Society of Japan –Celebrating the RSJ's 20th Anniversary–* (2002), 3C21 (CDROM).

Journal paper:

3. A. Takanishi, Quasi Dynamic Walking of the Biped Walking Robot (in Japanese), *Journal of the Robotics Society of Japan*, Vol. 1, No. 3, pp. 36–43,(1983).

Proceedings:

4. H. Yamato et al. Three Dimensional Biped Locomotion on Legged Mobile Robot (in Japanese), in *The 16th Annual Conference of the Robotics Society of Japan* (1998), Vol.16th, No. 3, pp. 1107-1108.

Journal paper:

5. T. Furuta et al. Biped Walking in a Humanoid Robot using Vertual Inverted Pendulum Model –Towards Realization of Natural Walking–, *A.C.C*, Vol. 2,pp. 515–517, (1997).

Proceedings:

6. K. Toda et al. Stabilization of Biped Locomotion utilizing Compensation in Double-Supporting Phase, in *Space 2002 & Robotics 2002 (Robotics 2002: The 5th International Conference and Exposition on Robotics for Challenging Situations and Environments)* (2002), pp. 409–415.

Journal paper:

7. Vukobratovic M. et al. On the Stability of Biped Locomotion, *IEEE Transactions On Bio-Mechanical Engineering 1970*, Vol. BME-17, No. 1, pp. 25–36, (1970).

Journal paper:

8. S. Kajita, Zero-Moment Ponint (ZMP) and Walking Control (in Japanese), *Journal of the Robotics Society of Japan*, Vol. 20, No. 3, pp. 229–232, (2002).

Journal paper:

9. A. Sano et al. Control of torque distribution in biped systems during double-support phase (in Japanese), *Transactions of the Society of Instrument and Control Engineers*, Vol. 26, No. 9, pp. 1066–1073, (1990).

Proceedings:

10. K. Nishiwaki et al. Online Generation of Desired Walking Pattern by Dynamically Stable Mixture and Connection of Pre-designed Motions (in Japanese), in *The 18th Annual Conference of the Robotics Society of Japan*(2000), Vol. 18, No. 3, pp. 1473–1474.

Proceedings:

11. T. Furuta et al. Design and Construction of a Series of Compact Humanoid Robots and Development of Biped Walk Control Strategies, in *International Conference on Humanoid Robots (HUMANOIDS 2000)*(2000) , 84.

Kengo TODA received his B.Eng. in Mechanical Engineering at Aoyama Gakuin University, in 2000. He is a Research Associate at the Department of Integrated Information Technology from 2001. Presently he studies on a humanoid project namely "Adaptive Whole-Body Motion Generation Based on Sensor-Based Control."

His research interests include every component technology of humanoid robotics, such as synchronized dynamic whole-body control, machine vision, behavior generation and integration of all of them.

Mizuki SAGARA received her B.Eng. and M.S. degrees in Mechanical Engineering from Aoyama Gakuin University, Japan in 2002 and 2004. She is currently an engineer at Optics and Sensors Product Division, Schlumberger Company and doing research on inflow measurement devices.

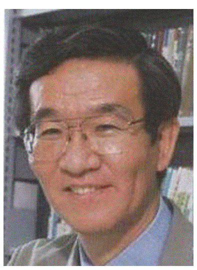

Ken TOMIYAMA obtained his Ph.D. in System Science at UCLA in 1977. He was Assistant Professor of the Department of Electrical Engineering at the University of Texas at El Paso form 1978 to1982 and at Pennsylvania State University from 1982 to 1988, then Associate Professor at the Department of Mechanical Engineering from 1988 to 1991 and Professor from 1991 to 2000. He is Professor of the Department of Integrated Information Technology, Aoyama Gakuin University, since 2000.

He is interested in all component of robotics, such as intelligent control, machine vision, behavior generation, and integration of them. His interests also include welfare robotics, intelligent manugfacturing systems and application of NN and GA to those fields.